Stereo Vision-based Autonomous Target Detection and Tracking on an Omnidirectional Mobile Robot

Wei Luo[a], Zhefei Xiao[b], Henrik Ebel[c] and Peter Eberhard[d]
Institute of Engineering and Computational Mechanics,
University of Stuttgart, Pfaffenwaldring 9, 70569 Stuttgart, Germany

Keywords: Autonomous System, Target Detection, Target Tracking, Stereo Vision, Mobile Robot.

Abstract: In this paper, a mobile robot equipped with an onboard computing unit and a stereo camera for autonomous target detection and tracking is introduced. This system can figure out an interesting target and track it robustly in real time. It is based on the ROS framework and can handle multi-resource information, such as RGB images, depth information, and IMU data. To balance the performance of the machine learning based object detection algorithm and the algorithm for object tracking, the Hamming distance and the intersection over union are selected as criteria. The performance of the system is verified in a hardware experiment in two typical scenarios.

1 INTRODUCTION

Mobile robots are among the vital investigation topics of robotics research. Mobile robots have been widely deployed in many applications, such as resource mining (Martins et al., 2018), security patrolling (Lopez et al., 2017), mapping (Fu et al., 2015) and object transportation (Kume et al., 2001). To accomplish these tasks autonomously, one of the critical challenges is to locate the robot's target in a complex environment and to robustly track it or even estimate its position based on information from onboard sensors. In some of the previous works, the mobile robots are equipped with a simple processing unit that cannot itself handle in real time complex sensor information such as laser or image data. Therefore, communication between the mobile robot and a more powerful remote controller is necessary during operation, which limits the practical application of the mobile robot in the real world.

With the recent years' rapid progress of machine learning, object detection does not need to rely only on predefined visual cues, such as colors (Li et al., 2014), shapes (Gode and Khobragade, 2016) or even templates (Kim et al., 2012), but can also be learned from large amounts of labeled data. State-of-the-art convolutional neural networks such as YOLO (Redmon and Farhadi, 2018), SSD (Liu et al., 2016) and R-CNN (Ren et al., 2017) perform favorably in multi-class object detection tasks with a high confidence level, and they can be further used as a backbone for learning new features or classes using transfer learning (Shao et al., 2015). Some works even use machine learning methods not only to detect, but also to track the objects. However, in general, this requires high computing power and is thereby a limitation on the applicability on embedded systems (Chang et al., 2018).

Different from convolutional neural network based object detection algorithms, typical object tracking algorithms in computer science focus on distinguishing between the target and the background. The tracking algorithms usually run faster than the machine learning-based algorithms, and they do not rely on a specialized processing unit to be real-time applicable. Several typical algorithms, such as kernel correlation filter (KCF) (Henriques et al., 2015), scalable part-based background-aware correlation filter (Fu et al., 2018) and tracking learning detection (TLD) (Kalal et al., 2012), run extremely fast with high tracking accuracy. Even so, these tracking algorithms have their own limitations. One of them is that they need to be provided with initial ground truth information since they cannot self-reliantly figure out which target they are tracking. Therefore, they require

[a] https://orcid.org/0000-0003-4016-765X
[b] https://orcid.org/0000-0002-1106-614X
[c] https://orcid.org/0000-0002-2632-6960
[d] https://orcid.org/0000-0003-1809-4407

Luo, W., Xiao, Z., Ebel, H. and Eberhard, P.
Stereo Vision-based Autonomous Target Detection and Tracking on an Omnidirectional Mobile Robot.
DOI: 10.5220/0007835702680275
In *Proceedings of the 16th International Conference on Informatics in Control, Automation and Robotics (ICINCO 2019)*, pages 268-275
ISBN: 978-989-758-380-3

an explicit identification of the initial target position and can hardly autonomously recover once the target is lost.

In the area of target detection and tracking, most of the previous works focus on feature-based object detection and tracking in the image plane (Li et al., 2017). In this paper the approach for object detection and object tracking is modified compared to the state-of-the-art methods and the system balances the performance autonomously depending on the selected criteria. Based on the detection and tracking results, the omnidirectional mobile robot detects and tracks the interesting target using a stereo camera and the onboard processing unit.

The paper is organized as follows. Section 2 describes the modeling of the mobile robot, the perception and projection of the stereo camera, and the criteria for the switching between tracking and detection. In Section 3, the structure of the autonomous target detection and tracking system and their specific properties are introduced. In Section 4, two typical scenarios are set up to verify the performance of the whole system. Finally, discussions and conclusions are presented in Section 5.

2 DEFINITION AND METHOD

2.1 Modeling of the Omnidirectional Mobile Robot and its Sensor System

The omnidirectional mobile robots used in this paper are Robotinos from Festo. The Robotino is a holonomic mobile robot with three omnidirectional-directional wheels, which have angles of 120° between each other, as illustrated in Fig. 1.

The subscript I indicates the inertial frame of reference. The coordinate system with subscript b is located in the middle of the mobile robot. Meanwhile, a stereo camera is fixed on the top of the mobile robot with camera coordinates marked with the subscript c.

With this model, the kinematic relationship between the wheel rotation speed ω_i and the global velocity $\dot{\boldsymbol{r}}_\mathrm{I}$ can be defined by

$$\dot{\boldsymbol{r}}_\mathrm{I}(t) = \begin{bmatrix} \dot{x}_\mathrm{I}(t) \\ \dot{y}_\mathrm{I}(t) \\ \dot{\theta}_\mathrm{I}(t) \end{bmatrix} = \begin{bmatrix} \cos(\theta_\mathrm{I}(t)) & -\sin(\theta_\mathrm{I}(t)) & 0 \\ \sin(\theta_\mathrm{I}(t)) & \cos(\theta_\mathrm{I}(t)) & 0 \\ 0 & 0 & 1 \end{bmatrix} R_\mathrm{w} \begin{bmatrix} -\frac{1}{\sqrt{3}} & 0 & \frac{1}{\sqrt{3}} \\ \frac{1}{3} & -\frac{2}{3} & \frac{1}{3} \\ \frac{1}{3L} & \frac{1}{3L} & \frac{1}{3L} \end{bmatrix} g \begin{bmatrix} \omega_1 \\ \omega_2 \\ \omega_3 \end{bmatrix}, \tag{1}$$

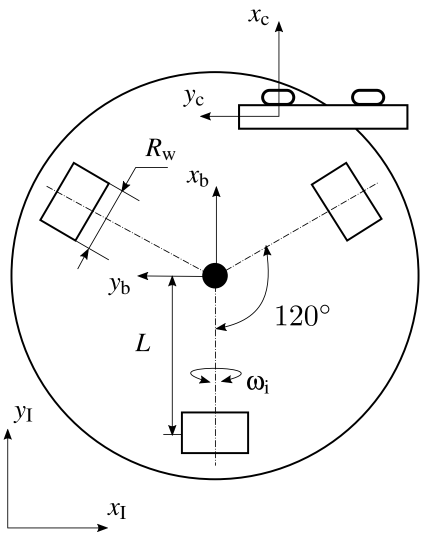

Figure 1: Robot geometry and employed coordinate systems.

where R_w is the wheel radius, and L is the distance between the rotation center of the Robotino and the centers of the wheels. The angle $\theta_\mathrm{I}(t)$ is the rotation angle around the z_b-axis. The constant $g := 1/16$ is the gear ratio.

Using odometry, one can obtain the position of the robot over a particular time interval $[t_\mathrm{k}, t_\mathrm{n}]$ by means of

$$\boldsymbol{r}_\mathrm{I}(t_n) = \begin{bmatrix} x_\mathrm{I}(t_k) \\ y_\mathrm{I}(t_k) \\ \theta_\mathrm{I}(t_k) \end{bmatrix} + \int_{t=t_k}^{t=t_n} \begin{bmatrix} \dot{x}_\mathrm{I}(t) \\ \dot{y}_\mathrm{I}(t) \\ \dot{\theta}_\mathrm{I}(t) \end{bmatrix} \mathrm{d}t. \tag{2}$$

However, due to wheel slip and other disturbances, an error is introduced that will be integrated over time and it is thus expected to increase with time. Therefore, to gain a more precise localization of the robot in the experiment, some additional data can be fused using a Kalman filter. One localization information comes from an external camera with the support from ARToolKit. To that end, on top of the robot, a predefined marker is attached and its location and orientation are determined relative to a marker fixed on the ground that represents the inertial frame of reference. The second data source for data fusion can be obtained from the inertial measurement unit (IMU) of the ZED Mini stereo camera. This camera has a built-in IMU which has the same coordinate system as the left camera, seen in Fig. 1, and it can provide the acceleration along the camera axes.

2.2 Perception and Projection

In this paper, a stereo camera is utilized for observing the environment and detecting the target. Compared with a single camera, the stereo camera does not only provide a 2D image but also a depth image, which can be used to estimate the 3D position of the target (Sharma et al., 2018).

The relationship between the target position in the inertial frame and the pixel position in the image coordinate frame is illustrated in Fig. 2.

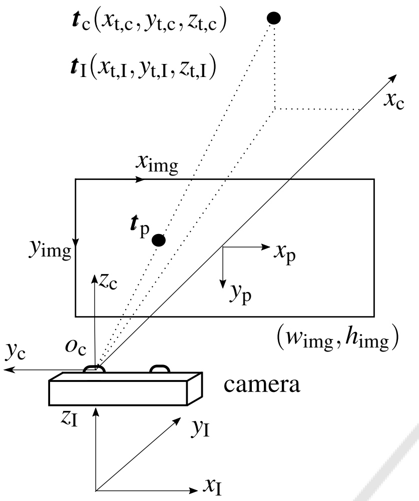

Figure 2: Target projection in pixel-, camera- and inertial coordinate frames.

Subsequently the applied target detection or tracking algorithms deliver the target's position (u, v) in the image frame $(x_{\rm img}, y_{\rm img})$ in pixel units. This pixel position can be transformed into the image coordinate frame through the equations

$$\begin{aligned} x_{\rm t,p} &= (u - \frac{w_{\rm img}}{2})\, c_{\rm P}, \\ y_{\rm t,p} &= (v - \frac{h_{\rm img}}{2})\, c_{\rm P}, \end{aligned} \tag{3}$$

yielding the target position $\boldsymbol{t}_{\rm p}$, and where $c_{\rm P}$ is the pixel size by resolution and $w_{\rm img}$ and $h_{\rm img}$ are the numbers of pixels in horizontal and vertical directions, respectively.

Furthermore, the stereo camera provides depth information corresponding to pixel coordinates in the form (u, v, d). The value of d is the distance between the object and the camera plane. Therefore, the projection of the target in camera coordinate $x_{\rm c}$ is equal to d. Thus, according to the triangle similarity, the target position $\boldsymbol{t}_{\rm c}$ to the camera coordinates can be estimated through

$$\begin{aligned} x_{\rm t,c} &= d, \\ y_{\rm t,c} &= -\frac{x_{\rm t,p}}{f} x_{\rm t,c}, \\ z_{\rm t,c} &= -\frac{y_{\rm t,p}}{f} x_{\rm t,c}, \end{aligned} \tag{4}$$

where f is the focal length of the stereo camera. Considering the offset and rotation between camera frame and inertial frame, the target position $\boldsymbol{t}_{\rm I}$ in the inertial frame can be obtained by

$$\begin{bmatrix} x_{\rm t,I} \\ y_{\rm t,I} \\ z_{\rm t,I} \end{bmatrix} = \boldsymbol{R}_{\rm Ib} \left(\boldsymbol{R}_{\rm bc} \begin{bmatrix} x_{\rm t,c} \\ y_{\rm t,c} \\ z_{\rm t,c} \end{bmatrix} + \boldsymbol{r}_{\rm camera,b} \right) + \boldsymbol{r}_{\rm m,\, I} \tag{5}$$

in which $\boldsymbol{R}_{\rm Ib}$ is the coordinate transformation from the mobile robot frame to inertial frame, and $\boldsymbol{R}_{\rm bc}$ denotes the rotation matrix between the mobile robot frame and the camera frame, which is an identity matrix according to the coordinate system definition in Fig. 1. Furthermore, the position of the camera frame in the robot frame is given by $\boldsymbol{r}_{\rm camera,b}$, while the robot position in the inertial frame is denoted by $\boldsymbol{r}_{\rm m,I}$.

2.3 Criteria for Autonomous Switching between Tracking and Detection

As usual, the tracking algorithms consume less computing power compared with machine learning-based object detection methods. Hence, to achieve satisfactory sampling rates, it is crucial that one executes the tracking algorithm most of the time as long as it works properly. However, the tracking algorithm may be mislead by other objects appearing in the view of the camera. For instance, when an other object is moving through the image and even just briefly blocks the target in the view of the mobile robot, or when the target moves behind some obstacles, the tracking algorithm may identify a wrong object and may never recover. Therefore, these situations need to be automatically recognized by the robot, so that it can employ an object detection algorithm to reacquaint the target. However, the object detection algorithms have a lower update rate than the tracking algorithms and should hence only be executed when necessary to obtain optimal performance.

To that end, it is necessary to figure out some criteria to make a switching from tracking to detection and vice versa according to the target state during the mission. In this paper, the intersection over union and the Hamming distance are chosen to handle this problem.

2.3.1 Intersection over Union

The intersection over union (IoU) is a typical criterion for object detection in computer science. Usually, it compares the estimated result with the ground truth and returns the difference as a loss criterion. In the application of this paper, there is no ground truth predefined manually. The comparison takes place between the target zone in the current image frame and the previously estimated target zone in the image frame. To estimate the IoU, one calculates the ratio between the area of the intersection and the area of union of the two target zones. The intersection area is marked with a chess board pattern in the example illustrated in Fig. 3. The ratio is given by using the following equation for two target zones

$$IoU_{\mathrm{i}} = \frac{\text{target zone}_{\mathrm{i}} \cap \text{target zone}_{\mathrm{i-1}}}{\text{target zone}_{\mathrm{i}} \cup \text{target zone}_{\mathrm{i-1}}}, \; IoU_{\mathrm{i}} \in [0,1]. \tag{6}$$

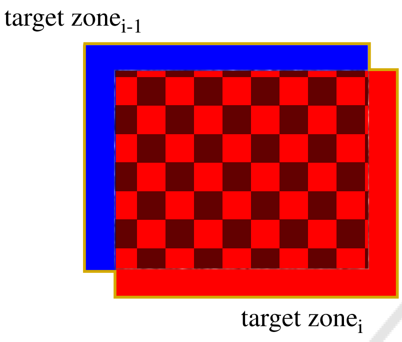

Figure 3: The intersection and the union areas between the image frame i and image frame i − 1.

Typically, the result from Eq. 6 should be close to 1, if the system has a high update rate, and hence, in two subsequent images, the estimated target should be located in a similar pixel position. When the system tracks the wrong object, the predicted location of the target may vary rapidly and reduce the IoU significantly. With this criterion, one can effectively detect an unusual tracking performance and indicate to the system to reinitialize by means of target detection.

2.3.2 Hamming Distance

Apart from calculating the position change of the target zone, the content of the zone should also be inspected. In this paper, the Hamming distance is used as another criterion for judging the performance of the system (Hamming, 1950). The Hamming distance in this paper calculates the summation of the difference between two target images' feature maps pixel by pixel. If two images have a relatively large Hamming distance, these two images may have recorded different objects, which means the system has tracked a wrong target.

To generate the feature map, the perceptual hash (pHash) algorithm is utilized. First of all, the original target zone is compressed into a relatively small size, for instance 8×8 pixels, and converted from RGB to the monochrome form. Then, the pHash algorithm computes the features of the compressed target image depending on the discrete cosine transform (Ahmed et al., 1974). After gathering the image feature for each pixel, the pHash algorithm creates an empty feature map with the same size as the compressed target image, and then it marks the pixel with 1 in the feature map when the feature value on this pixel is above the average of the whole image features.

3 AUTONOMOUS TARGET DETECTION AND TRACKING SYSTEM

3.1 Hardware Setup

In this paper, an autonomous target detection and tracking system is built based on the omnidirectional mobile robot Robotino, see Fig 4.

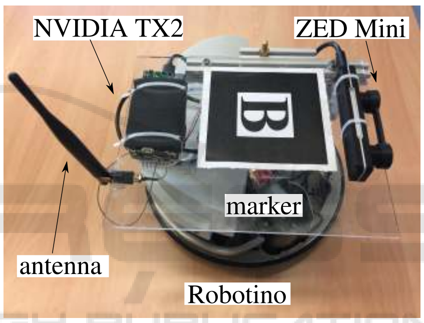

Figure 4: Hardware setup.

In the front of the Robotino a ZED Mini stereo camera from Stereolabs is mounted on an acrylic platform. It can simultaneously provide RGB images, depth image and point clouds at around 100 Hz, as well as the acceleration information at up to 800 Hz. Furthermore, an NVIDIA TX2 with a J120 carrier board from Auvidea is attached on the acrylic platform. This module has an embedded GPU unit and can handle directly the trained neural network using GPU-accelerated libraries. By combing the designed hardware, the streamed data from the ZED Mini camera as well as all necessary algorithms can be run in real-time directly onboard. Additionally, a marker is placed on top of the Robotino and the localization system, that is based on ARToolKit, can send the robot's real-time position wirelessly through LCM (Huang et al., 2010) or ROS.

3.2 System Setup

Based on the hardware above, the autonomous target detection and tracking system is deployed and organized under the ROS environment. There are five main functional blocks, and each functional block is named ‘node’ in ROS. The whole system setup is illustrated in Fig. 5.

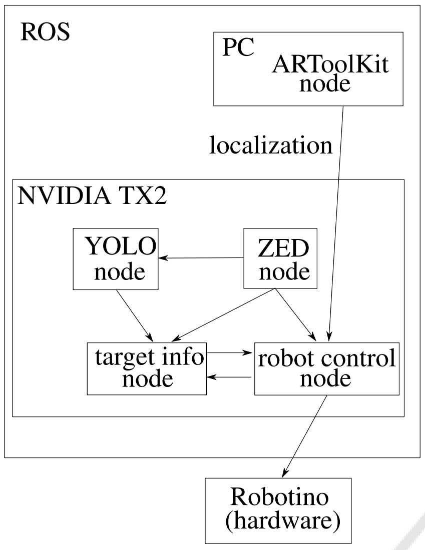

Figure 5: System setup.

To obtain the mobile robot’s global position, an external PC which connects a camera fixed to the ceiling is required. Based on the ARToolKit, this node calculates the Robotino’s pose using the markers in the test field and broadcasts the robot position and orientation at 10 Hz in the ROS network.

The ZED node is modified from the official ZED ROS package. It is a hardware correlative node, which is connected with the ZED Mini camera and advertises the RGB images, the depth images, the point clouds and the IMU data topics in ROS for other nodes during the operation.

To detect the target during the operation, a machine learning framework called YOLO is utilized as a backbone. YOLO is one of the state of art object detection frameworks and it has shown its performance for ImageNet/Coco datasets (Redmon and Farhadi, 2018). Meanwhile, it balances well the recognition speed and the prediction accuracy compared with other object detection algorithms. These features are essential not only for traditional object detection tasks in computer science but also in robotics, since the robot is sensitive to operation delays. Without loss of generality, in the context of this paper, the target to be detected and tracked is also a Robotino. Initially, the publicly available, pre-trained YOLO model cannot recognize Robotinos since a Robotino does not appear in the open dataset. Therefore, based on the pre-trained YOLO model and newly collected Robotino images, the modified YOLO model using transfer learning methods is trained for the demonstration. The YOLO node is recomposed on the basis of (Bjelonic, 2018). It imports the compressed RGB image from the ZED node and determines whether there is a target in front of the mobile robot, and then broadcasts the target’s position in the image coordinate system as well as the estimated confidence into the ROS network.

The main component in this system is the target info node. In this node, the necessary data are asynchronously collected from the YOLO node and the ZED node, respectively. To handle the data and obtain the target information for the further process, two threads are parallelly set up in this node. One main thread handles the target related information and estimates the target position in the inertial frame. The other thread serves as an action server and responds to all external requests for target states.

In the main thread, a target estimation algorithm is executed to obtain the target position in the image frame, see Algorithm 1. At first, the algorithm waits for the initial target detection from the YOLO node, since the tracking algorithm always requires a ground truth for the initialization. Once it gets a confirmation, the cropped target image will be passed on to the tracking algorithm, where, in this paper, the KCF algorithm is utilized as a standard tracking method (Henriques et al., 2015). In each loop, the process will update the target’s features depending on the current vision from ZED node. Compared with using only the tracking method, at the end of each loop, the performance of the tracking method is checked by means of the Hamming distance and the intersection over union of the current and the last target image. If the evaluation is beyond the allowed limits, the process will require a reinitialization for the tracking algorithm. Since only object detection can figure out the target from the camera image, the process will ask the YOLO node about the target’s position depending on the YOLO result. If YOLO can find the current target position, the process will take the new position to reinitialize the tracking algorithm. If both YOLO and KCF have totally lost the target, the node marks a label to warn the other components in system that there is no available target position currently. In the action thread, the results from the main thread will be further processed to obtain the distance to target and the target position in the global frame according to the task requirement.

The last component is to control the Robotino hardware depending on its global localization, the target states, and the depth image from the ZED node. This node consists of two threads simultaneously. The driving thread sends the robot’s current global local-

Algorithm 1: Target Estimation Algorithm.

```
 1: // Initialization
 2: repeat
 3:    inquiring the first target confirmation;
 4: until KCF is initialized
 5: // Main while loop
 6: while mission in process do
 7:    if reInit = 0 then
 8:       updateKCF();
 9:       $hash_{cur}$ = pHash($image_{cur}$);
10:       distance = HammingDistance
          ($hash_{cur}$, $hash_{prev}$);
11:       iou_result = IOU($image_{cur}$, $image_{prev}$);
12:       if distance or iou_result over the threshold
          then
13:          reInit = 1;
14:       else
15:          $hash_{prev}$ = $hash_{cur}$;
16:       end if
17:    else
18:       if YOLO result available then
19:          reInitKCF();
20:          reInit, fail_times and lost_target = 0;
21:       else if fail_times under the limitation then
22:          fail_times++ and reInit = 0;
23:       else
24:          lost_target = 1;
25:       end if
26:    end if
27: end while
```

ization to the action server into the target info node and waits for the response. Once the target's pixel position and the global localization are provided, the node connects to the Robotino using the Robotino API and drives the robot hardware. If there is any obstacle, detected from the depth image, in front of the robot by the second thread, the object detection function will lead the robot to avoid the obstacle if necessary.

4 EXPERIMENT

To verify the performance of the autonomous target detection and tracking system, two scenarios are set up in the experiment. There are two Robotinos in the field. One is the tracking robot, which is equipped with the autonomous detection and tracking system, the other is the target robot which moves along an arbitrary trajectory during the experiment.

To test the stability of the proposed system, the target robot follows a predefined square trajectory, while the tracking robot should lock onto the target robot, maintain it in the center of the view, and estimate its global position in the first scenario. In Fig. 6, four image outputs, which are recorded by the ZED left camera from the experiment are illustrated. In Fig. 6a, the object detection and tracking perform similarly, therefore, the algorithm updates the target position using the tracking algorithm. In some cases, the object detection algorithm may not recognize the target robot, e.g., under low light or low contrast conditions, for instance, in the scene in Fig. 6b. In this situation, the system can update solely using the tracking algorithm. When the tracking algorithm cannot properly track the target, as seen in Fig. 6c, the system evaluates the performance of the tracking algorithm and autonomously corrects the tracking result using the detection algorithm and reinitialize the tracking model, see Fig. 6d. Meanwhile, both the referenced trajectory recorded by the ARToolKit and the estimated trajectory target position from the system are illustrated in Fig. 7. The performance of the position estimation is evaluated through the root mean square error (RMSE) through

$$RMSE = \sqrt{\frac{\sum_i (x_{ref,i} - x_{est,i})^2 + (y_{ref,i} - y_{est,i})^2}{n}}. \quad (7)$$

During the experiment, the system can stably lock onto the target robot and the RMSE of the position estimation in the experiment is around 0.1 m.

In the second scenario, the dynamic performance of the proposed system is verified. In this task, the tracking robot needs to detect and follow the target robot, while avoiding obstacles at the same time. In the middle of the scenario, there are two obstacles that may block the target robot from the tracking robot's view. Therefore, the system has the ability to regain the target position and resume the tracking procedure once the target is lost. The scenario setup and the trajectories of both robots and the estimated target are illustrated in Fig. 8. At the beginning of the experiment, the tracking robot will turn to the target and shorten the distance between itself and the target, once the target is found. After a short movement, the system detects the obstacle in the view, which may cause a collision. Therefore, the system drives the tracking robot away from the obstacle preferentially. Furthermore, for testing the performance and robustness of the system, the target robot moves and tries to hide behind the obstacle, as seen in Fig. 9. If the target is out of the camera range, e.g., the scene in Fig. 9b, the system analyzes the feedback from the target info node and drives the tracking robot to go to the last estimated target position in the global coordinate frame. Then, it executes a search process until the target robot appears again in the view.

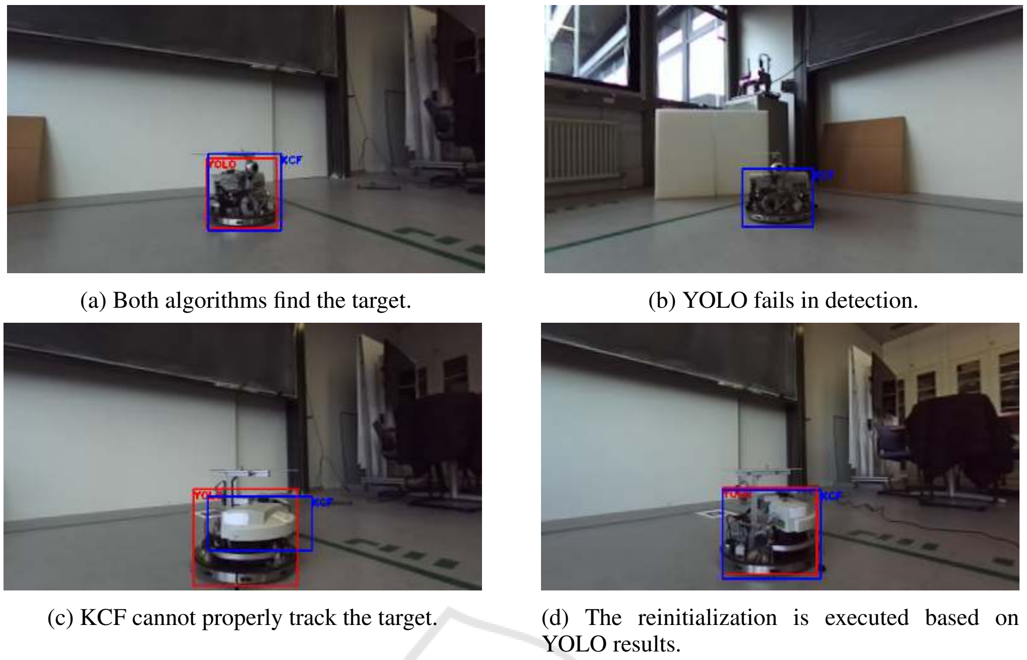

(a) Both algorithms find the target.

(b) YOLO fails in detection.

(c) KCF cannot properly track the target.

(d) The reinitialization is executed based on YOLO results.

Figure 6: Four image outputs from the first scenario, as recorded by the left ZED camera.

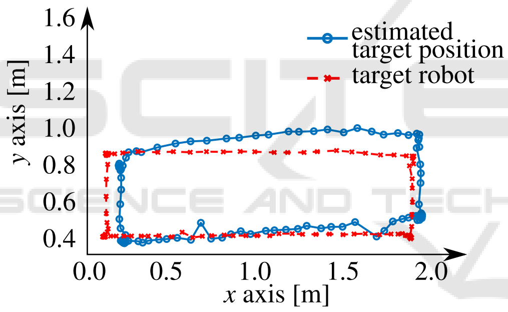

Figure 7: Trajectories of the estimated target position and the real target position in the first scenario.

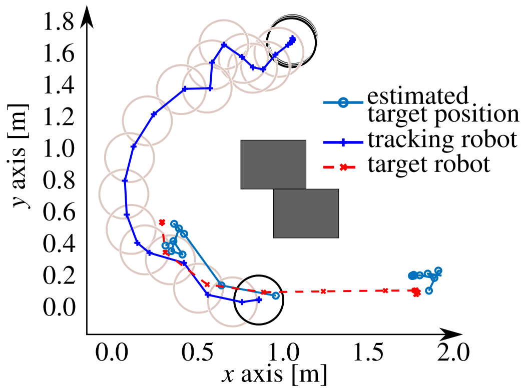

Figure 8: Trajectories of the tracking robot, the target robot and the estimated target robot position in the second scenario.

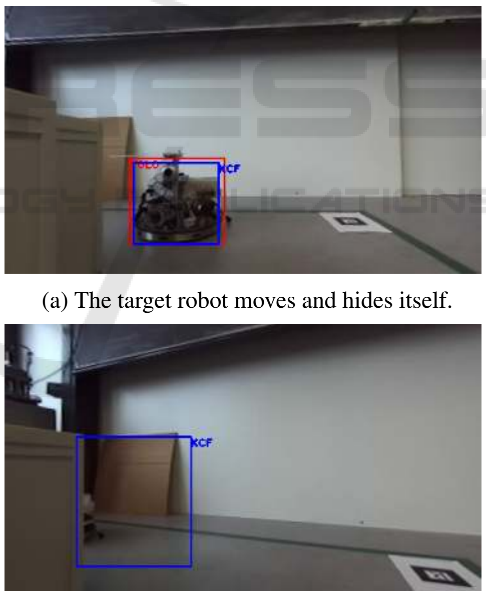

(a) The target robot moves and hides itself.

(b) The target is beyond the view of the camera.

Figure 9: Two image outputs from the second scenario.

5 CONCLUSIONS

In this paper, an autonomous target tracking and detection system is designed and implemented on an omnidirectional mobile robot. Based on the evaluation of the Hamming distance and the intersection over union, the system orchestrates the detection and tracking algorithms within the ROS environment. During the experiment, the system can guide the tracking robot to find the target robustly in real time. Furthermore, with the stereo vision, the system also has the ability to estimate the target's position using depth information which can drive the robot to track and get close to the target. In future work, more criteria can be chosen and tested within the system. Furthermore, it seems promising to train a recurrent neural network to potentially gain a better detecting and tracking performance.

ACKNOWLEDGEMENTS

This research benefited from the support by the China Scholarship Council (CSC, No. 201808080061) for Wei Luo.

REFERENCES

Ahmed, N., Natarajan, T., and Rao, K. R. (1974). Discrete cosine transform. *IEEE Transactions on Computers*, C-23(1):90–93.

Bjelonic, M. (2016–2018). YOLO ROS: Real-time object detection for ROS. https://github.com/leggedrobotics/darknet_ros.

Chang, Y., Chung, P., and Lin, H. (2018). Deep learning for object identification in ROS-based mobile robots. In *IEEE International Conference on Applied System Invention (ICASI)*, pages 66–69, Chiba, Japan.

Fu, C., Carrio, A., and Campoy, P. (2015). Efficient visual odometry and mapping for unmanned aerial vehicle using arm-based stereo vision pre-processing system. In *International Conference on Unmanned Aircraft Systems (ICUAS)*, pages 957–962, Denver, USA.

Fu, C., Zhang, Y., Duan, R., and Xie, Z. (2018). Robust scalable part-based visual tracking for UAV with background-aware correlation filter. In *IEEE International Conference on Robotics and Biomimetics (ROBIO)*, pages 1–8, Kuala Lumpur, Malaysia.

Gode, C. S. and Khobragade, A. S. (2016). Object detection using color clue and shape feature. In *International Conference on Wireless Communications, Signal Processing and Networking (WiSPNET)*, pages 464–468, Chennai, India.

Hamming, R. W. (1950). Error detecting and error correcting codes. *The Bell System Technical Journal*, 29(2):147–160.

Henriques, J. F., Caseiro, R., Martins, P., and Batista, J. (2015). High-speed tracking with kernelized correlation filters. *IEEE Transactions on Pattern Analysis and Machine Intelligence (TPAMI)*, 37(3):583–596.

Huang, A. S., Olson, E., and Moore, D. C. (2010). LCM: Lightweight communications and marshalling. In *IEEE/RSJ International Conference on Intelligent Robots and Systems (IROS)*, pages 4057–4062, Taipei, Taiwan.

Kalal, Z., Mikolajczyk, K., and Matas, J. (2012). Tracking-learning-detection. *IEEE Transactions on Pattern Analysis and Machine Intelligence (TPAMI)*, 34(7):1409–1422.

Kim, D., Lee, D., Myung, H., and Choi, H. (2012). Object detection and tracking for autonomous underwater robots using weighted template matching. In *Oceans - Yeosu*, pages 1–5, Yeosu, South Korea.

Kume, Y., Hirata, Y., Kosuge, K., Asama, H., Kaetsu, H., and Kawabata, K. (2001). Decentralized control of multiple mobile robots transporting a single object in coordination without using force/torque sensors. In *IEEE International Conference on Robotics and Automation (ICRA)*, volume 3, pages 3004–3009 vol.3, Seoul, South Korea.

Li, J., Wang, J., and Mao, J. (2014). Color moving object detection method based on automatic color clustering. In *Proceedings of the 33rd Chinese Control Conference (CCC)*, pages 7232–7235, Nanjing, China.

Li, K., Zhao, X., Sun, Z., and Tan, M. (2017). Robust target detection, tracking and following for an indoor mobile robot. In *IEEE International Conference on Robotics and Biomimetics (ROBIO)*, pages 593–598, Macau, China.

Liu, W., Anguelov, D., Erhan, D., Szegedy, C., Reed, S., Fu, C.-Y., and Berg, A. C. (2016). SSD: Single shot multibox detector. In Leibe, B., Matas, J., Sebe, N., and Welling, M., editors, *European Conference on Computer Vision (ECCV)*, pages 21–37, Amsterdam, the Netherlands.

Lopez, A., Paredes, R., Quiroz, D., Trovato, G., and Cuellar, F. (2017). Robotman: A security robot for human-robot interaction. In *18th International Conference on Advanced Robotics (ICAR)*, pages 7–12, Hong Kong.

Martins, A., Almeida, J., Almeida, C., Dias, A., Dias, N., Aaltonen, J., Heininen, A., Koskinen, K. T., Rossi, C., Dominguez, S., Vörös, C., Henley, S., McLoughlin, M., van Moerkerk, H., Tweedie, J., Bodo, B., Zajzon, N., and Silva, E. (2018). UX 1 system design - a robotic system for underwater mining exploration. In *IEEE/RSJ International Conference on Intelligent Robots and Systems (IROS)*, pages 1494–1500.

Redmon, J. and Farhadi, A. (2018). Yolov3: An incremental improvement. *CoRR*, arxiv.org/abs/1804.02767.

Ren, S., He, K., Girshick, R., and Sun, J. (2017). Faster R-CNN: Towards real-time object detection with region proposal networks. *IEEE Transactions on Pattern Analysis and Machine Intelligence*, 39(6):1137–1149.

Shao, L., Zhu, F., and Li, X. (2015). Transfer learning for visual categorization: A survey. *IEEE Transactions on Neural Networks and Learning Systems*, 26(5):1019–1034.

Sharma, T. G., Kritin Valivati, N., Puthige, A., and Hari, U. (2018). Object position estimation using stereo vision. In *IEEE 8th International Advance Computing Conference (IACC)*, pages 66–71, Greater Noida, India.